CPC(HEP & NP), 2010, **34**(4): 427–432 Chinese Physics C Vol. 34, No. 4, Apr., 2010

Study of new boson $W_1^{\pm}$ in the Minimal Higgsless Model at the LHC*

ZHANG Zhen-Xia(张振霞)[1;1)] BIAN Jian-Guo(卞建国)[1] CHEN Guo-Ming(陈国明)[1]
CHEN Ming-Shui(陈明水)[1] LI Zu-Hao(李祖豪)[1] LIANG Song(梁松)[1] MENG Xiang-Wei(孟祥伟)[1]
QI Yong-Hui(祁永辉)[3] TANG Zhi-Cheng(唐志成)[1] TAO Jun-Quan(陶军全)[1] WANG Jian(王健)[1]
WANG Jian(王健)[2] WANG Zheng(王征)[1] WANG Xian-You(汪先友)[4] WANG Jian-Xiong(王建雄)[1]
XIAO Hong(肖虹)[1] YANG Min(杨民)[1] ZANG Jing-Jing(臧晶晶)[1]
ZHANG Bin(张斌)[3] ZHANG Zhen(张震)[1]

[1] Institute of High Energy Physics, Chinese Academy of Sciences, Beijing 100049, China
[2] Graduate University of Chinese Academy of Sciences, Beijing 100049, China
[3] Center for High Energy Physics, Tsinghua University, Beijing 100084, China
[4] Theoretical Physics Institute, Chongqing University, Chongqing 400044, China

Abstract The Minimal Higgsless Model predicts the existence of new vector gauge boson $W_1^{\pm}$. By the process $PP \rightarrow W_1^{\pm}qq \rightarrow W^{\pm}Z^0qq$, $Z^0 \rightarrow l^+l^-$, $W^{\pm} \rightarrow qq$ (l=e,μ; q is hadronized to be jets), we study the sensitivity of searching for this possible vector gauge boson in the level of generator events of signal and backgrounds, then give integrated luminosity required to discover 5σ signal as a function of $W_1^{\pm}$ mass. The generator for the signal $PP \rightarrow W_1^{\pm}qq \rightarrow W^{\pm}Z^0qq$ at tree level is developed with the Minimal Higgsless Model and then interfaced with PYTHIA for the parton showers and hadronization. The backgrounds are produced with MadGraph and PYTHIA.

Key words Minimal Higgsless Model, $W_1^{\pm}$, sensitivity, integrated luminosity

PACS 12.60.Cn, 14.70.Pw

1 Introduction

The Higgs boson of the electroweak standard model has been sought in vain by all known experiments so far. The absence of such a Higgs boson will violate the perturbative unitarity of the high energy longitudinal weak boson scattering $V_LV_L \rightarrow V_LV_L$ ($V = W^{\pm}, Z^0$). To postpone this unitarity violation, the Higgsless models are proposed, in which the new spin-1 gauge bosons(rather than spin-0 Higgs scalars) play the key role in both 5d and 4d realizations [1].

Reference [2] presents the first LHC-study on the distinct signatures of the Minimal Higgsless Model which is exactly gauge-invariant and predicts just a pair of new gauge bosons ($W_1^{\pm}$, Z_1^0) as light as about 400 GeV.

The signature of new boson $W_1^{\pm}$ in the process $pp \rightarrow W^{\pm}Z^0qq \rightarrow \nu 3lqq$ and the process $pp \rightarrow W^{\pm}Z^0Z^0 \rightarrow qq4l (l = e, \mu)$ were investigated at the parton level, without the initial and final state parton showers and hadronization for the signal and backgrounds and only the background $pp \rightarrow W^{\pm}Z^0qq$ was considered. Assuming W_1 mass within the region of (400, 800) GeV, the integrated luminosity required for 5σ $W_1^{\pm}$ signal detection is from about 7/fb to 30/fb for the first channel, while it is from about 7.8/fb to 400/fb for the second channel [2]. Considering the initial and final state parton showers and hadronization, even some detector effects including pile-up, particle identity efficiency and so on, these two channels are also researched in Refs. [3, 4].

In this paper, we present the results on the study

Received 14 May 2009, Revised 8 September 2009
* Supported by NSFC (10435070, 10721140381, 10099630), China Ministry of Science and Technology (2007CB16101), CAS (KJCX2-N17, 1730911111) and China Postdoctoral Science Foundation (20090450577)
1) E-mail: zxzhang@mail.ihep.ac.cn

of $W_1^{\pm}$ production in the process $pp \to W_1^{\pm}qq \to W^{\pm}Z^0qq$, $W^{\pm} \to qq$ and $Z^0 \to l^+l^-$ by analyzing the fully hadronized events of the signal and backgrounds at the generator level. There are two leptons and four jets in the final states. The generator for the signal of this channel is developed based on the Minimal Higgsless Model and interfaced with PYTHIA [5] for the parton showers and parton hadronization. The Feynman diagram for the process $W_1^{\pm}$ production in the process $pp \to W_1^{\pm}qq \to W^{\pm}Z^0qq$, $W^{\pm} \to qq$ and $Z^0 \to l^+l^-$ is shown in Fig. 1, in which the intermediate state $W_1^{\pm}$ proceeds throught $W^{\pm}Z^0$ fusion. The typical cross sections (assuming m_{W_1} to be 550 GeV) are 48.74 fb and 27.68 fb for $pp \to W_1^{\pm}qq \to W^+Z^0qq \to l^+l^-4q$ and $pp \to W_1^{\pm}qq \to W^-Z^0qq \to l^+l^-4q$ respectively, and $\Gamma_{W_1^{\pm}} \approx 5$ GeV according to MHLM. According to MHLM, which consists of just three lattice sites (the Three Site Model) [6], the coupling of W_1 and $W^{\pm}Z^0$ only depends on the mass of W_1 in the computation of cross section, while in general MHLM it depends on the sum rule relation of the mass of W_1.

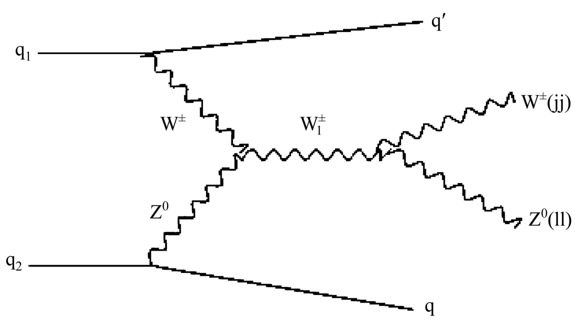

Fig. 1. Feynman diagram for the process $pp \to W^{\pm}Z^0qq \to l^+l^-jjjj$.

In this work, we consider the effects of parton showers and hadronization, initial and final state radiation, simulating more backgrounds. This work also considers some detector effects, such as the efficiencies of identifying electrons and muons, the energy resolutions of leptons and jets, and the effects of pile-up events at high LHC luminosities. These improvements add to the realism of the study.

2 Signal and background production

According to the matrix element calculation of the LHC process at a full tree level in the Minimal Higgsless Model by the authors of Ref. [2], we obtain the generator for the signal channel $pp \to W_1^{\pm}pp \to W^{\pm}Z^0qq \to l^+l^-4q$. Here the Parton Distribution Function (PDF) CTEQ6L [7] is used. In this work the same pre-selections at the parton level are used as those in Ref. [2]. Jets satisfy transverse momentum $P_t(j) > 15$ GeV and pseudo-rapidity $|\eta_j| < 4.5$. Leptons satisfy $P_t(l) > 10$ GeV, $|\eta_l| < 2.5$. The weighted parton-level events from the generator are fed into PYTHIA. The initial and final state showers and hadronization are done by PYTHIA.

The cross section after the pre-selection, the number of events produced and the event yields for 100 fb^{-1} are listed in Table 1, where the event yield is the events number of signal at luminosity of 100 fb^{-1}. The uncertainties of the cross section are discussed in Section 4.

Table 1. Production of signal sample $pp \to W_1^{\pm}pp \to W^{\pm}Z^0qq \to l^+l^-qqqq$. For each mass point, more than 4000 events are produced altogether for W_1^+ and W_1^-. $n_{W_1^+}$ and $n_{W_1^-}$ are different according to their cross sections. The sum of cross sections of W_1^+ and W_1^- is shown with the error statistically estimated from the PDF uncertainty.

$W_1^{\pm}$ mass/GeV	cross section/fb	events produced	event yield/(100 fb^{-1})
450	126.50± 31.73	4000	12650
500	78.13±14.37	4000	7813
550	76.42±10.20	7642	7642
600	49.07±6.53	4000	4907
650	30.23±7.11	4000	3023
700	28.82±5.87	4000	2882
750	21.80±1.05	4000	2180
800	18.81±1.20	4000	1881

There are two leptons ($l = e^{\pm}, \mu^{\pm}$) and four quarks in the signal process. Therefore the contamination to the signal process mainly comes from the processes including two leptons and multiple jets in the final state. In view of the final state of the signal process, the backgrounds include: (a) the SM production, $pp \to Z^0 + nj \to l^+l^- + nj$, $1 \leqslant n \leqslant 4$ (b) the SM $t\bar{t}$, $t \to bW^{\pm}$, (c) the SM process $pp \to jjZ^0Z^0 \to$

$jjjjl^+l^-$ with jj = qg, gg, qq, (d) the SM process $pp \to jZ^0Z^0 \to jjjl^+l^-$ with j = q, g, (e) the SM process $pp \to jjW^{\pm}Z^0 \to jjjjl^+l^-$, which is irreducible, (f) the SM process $pp \to W^+W^-Z^0 \to jjjjl^+l^-$, which also is irreducible, (g) the SM process $pp \to jW^{\pm}Z^0 \to jjjl^+l^-$. All the background channels listed above can make contamination to the signal because of their initial and final radiations, parton showers and their much large cross sections.

In this work, the backgrounds (a)–(g) are simulated using MadGraph [8] interfaced with PYTHIA [5]. The cross sections, the number of the events and the event yields of 100 fb^{-1} for the background samples are given in Table 2.

Table 2. Production of backgrounds. j represents a fundamental parton of flavors d, u, s, c, b, t, g.

process	cross section/fb	events produced	event yield/(100 fb^{-1})
Z^0j	1.248×10^6	10500000	124800000
Z^0jj	3.955×10^5	4000000	39550000
Z^0jjj	3.180×10^5	3717745	31800000
Z^0jjjj	2.324×10^4	228000	2324000
$t\bar{t}$	3.171×10^4	2923537	3171000
$W^{\pm}Z^0jj$	7.847×10^2	499918	778470
Z^0Z^0jj	5.365×10^3	408659	536500
Z^0Z^0j	7.662×10^3	432478	766200
$W^{\pm}Z^0j$	8.490×10^2	49993	84900
$W^+W^-Z^0$	2.987	9996	299

3 Event selection

The event selection is based on the features of the signal process. There are two leptons with high momentum and four hard partons in the final state. The two leptons come from Z^0 decay. Two of the four partons evolve into hard forward jets and the other two partons coming from $W^{\pm}$ also evolve into hard jets. The events are selected if there are two leptons with opposite charge and at least four jets in the final states. At the same time, the leptons are required to satisfy $P_t(l)>15$ GeV, $|\eta_l|<2.5$ and jets satisfy $P_t(j)>15$ GeV, $|\eta_j|<4.5$. Each jet is reconstructed with cone of $\delta R=\sqrt{\delta\eta^2+\delta\phi^2}=0.7$ and satisfies $\delta R(j,l)>0.3$ to suppress fake jets.

The jet reconstruction algorithm is one provided with PYTHIA [5], in which a detector grid is assumed, with the pseudo-rapidity range $|\eta|<\eta_{max}(4.5)$ and the full azimuthal range each divides into 50 equally large bins, giving a rectangular grid; the cell with the largest transverse energy E_T is taken as a jet initiator; a candidate jet is defined to consist of all cells which are within $(\eta-\eta_{initiator})^2+(\phi-\phi_{initiator})^2<\delta R^2$; the candidate jet is accepted if the summed E_T is above 7 GeV and all its cells are removed from future consideration; the sequence is now repeated within the remaining cell of the highest E_T and so on.

Z^0 reconstructed from l^+l^- is required to satisfy

$$|M_{l^+l^-}-91.18|<10 \text{ GeV} \quad (1)$$

We select two jets from four good jets to reconstruct $W^{\pm}$, here the two jets must satisfy $|\eta_j|<2.0$, the transverse momentum over momentum of each jet larger than 0.3, η difference between the two jets less than 1.5 and the transverse momentum difference between the two jets less than 250 GeV. The two jets with mass close to $W^{\pm}$ are used to reconstruct the invariant mass of $W^{\pm}$, which is required to be

$$|M_{W^{\pm}}-80.398|<20 \text{ GeV} \quad (2)$$

because of the worse resolution of jet reconstruction.

The two forward jets are selected from the jets satisfying $|\eta_j|>1.0$, the transverse momentum over momentum of each jet less than 0.3 and η difference between the two jets larger than 3.0 GeV. The invariant mass of the two forward jets is also required to be larger than 400 GeV. We think two jets with the largest sum of transverse momentum satisfying the above criteria as the two forward jets.

To suppress the backgrounds further more, especially the main background $pp\to Z^0+nj$, we required the maximum transverse momentum of four jets satisfy:

$$P_t(\max)(j)>100 \text{ GeV} \quad (3)$$

and the sum of transverse momentum of four jets satisfy:

$$\sum_{i=1}^{4}P_t(j_i)>300 \text{ GeV} \quad (4)$$

shown in Fig. 2 and Fig. 3 respectively.

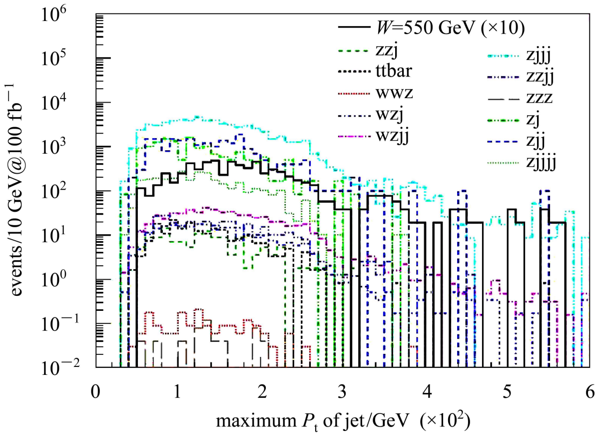

Fig. 2. Maximum transverse momentum of four jets for signal and backgrounds processes.

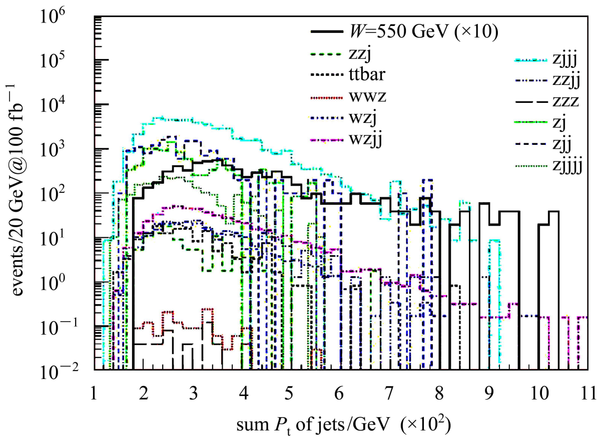

Fig. 3. Sum of transverse momentum of four jets for signal and backgrounds processes.

In lepton point of view, the sum of transverse momentum of two leptons is required:

$$\sum_{i=1}^{2} P_{\rm t}({\rm l}_i) > 160 \text{ GeV} \tag{5}$$

shown in Fig. 4.

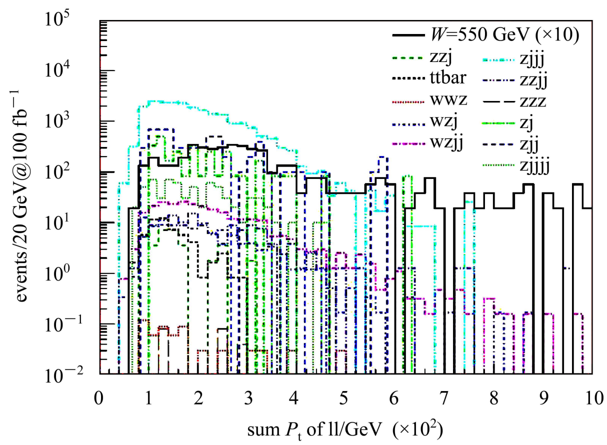

Fig. 4. Sum of transverse momentum of two leptons for signal and backgrounds processes.

In conclusion, the total numbers and efficiencies for some important cuts for the signal and background samples are shown in Table 3, where $W_1^{\pm}$ mass is 550 GeV.

Table 3. The cut flow. The luminosity is set to be 100 fb^{-1}. The second column is the number of events, the other columns are the remaining efficiencies after each cut. j represents a fundamental parton of flavors d, u, s, c, b, t, g.

cut	total events	$n_{\rm l}=2$	$n_{\rm j}\geqslant 4$	$M_{\rm W^{\pm}}=80\pm 20$	forward jets	max $P_{\rm tj}>100$	$\Sigma P_{\rm tj}>300$	$\Sigma P_{\rm tl}>160$
signal	7642	0.97	0.89	0.47	0.17	0.15	0.12	0.10
Z^0j	1.24×10^8	0.49	0.22	8.49×10^{-3}	6.8×10^{-4}	2.5×10^{-4}	5.8×10^{-5}	3.1×10^{-5}
Z^0jj	3.96×10^7	0.57	0.11	5.8×10^{-2}	3.6×10^{-3}	1.4×10^{-3}	4.2×10^{-4}	1.78×10^{-4}
Z^0jjj	3.18×10^7	0.48	0.22	0.11	9.8×10^{-3}	4.5×10^{-3}	1.8×10^{-3}	7.7×10^{-4}
Z^0jjjj	2.32×10^6	0.35	0.23	0.13	1.3×10^{-2}	4.1×10^{-3}	1.1×10^{-3}	5.4×10^{-4}
$t\bar{t}$	3.17×10^6	0.33	2.9×10^{-2}	1.8×10^{-2}	2.2×10^{-3}	9.7×10^{-4}	2.9×10^{-4}	3.9×10^{-5}
jjZ^0Z^0	5.37×10^5	8.2×10^{-2}	5.2×10^{-2}	3.5×10^{-2}	3.0×10^{-3}	1.5×10^{-3}	7.1×10^{-4}	3.2×10^{-4}
jZ^0Z^0	7.66×10^5	8.0×10^{-2}	2.9×10^{-2}	1.8×10^{-2}	1.0×10^{-3}	3.8×10^{-4}	1.3×10^{-4}	5.1×10^{-5}
$W^{\pm}Z^0$jj	7.79×10^5	6.4×10^{-1}	5.2×10^{-1}	3.4×10^{-1}	3.7×10^{-2}	2.1×10^{-2}	1.0×10^{-2}	4.8×10^{-3}
$W^+W^-Z^0$	299	6.6×10^{-1}	5.1×10^{-1}	3.8×10^{-1}	2.3×10^{-2}	1.2×10^{-2}	4.9×10^{-3}	2.2×10^{-3}
$W^{\pm}Z^0$j	8.49×10^4	6.1×10^{-1}	3.3×10^{-1}	2.0×10^{-1}	1.7×10^{-2}	8.6×10^{-3}	3.7×10^{-3}	1.8×10^{-3}

The spectrum of invariant mass of $W^{\pm}Z^0$ for signal and background samples are plotted in Fig. 5, after applying these cuts for an integrated luminosity of 100 fb^{-1}. These distributions of signal and background processes are plotted with stack. The peak with real line in mass region of 550 GeV is just the signal of new boson $W_1^{\pm}$. The largest background is Z^0jjj, then the second Z^0jj, from large to small there are still Z^0j, Z^0jjjj, $W^{\pm}Z^0$jj and so on. Here the signal is shown in the plot after multiplying 10 times.

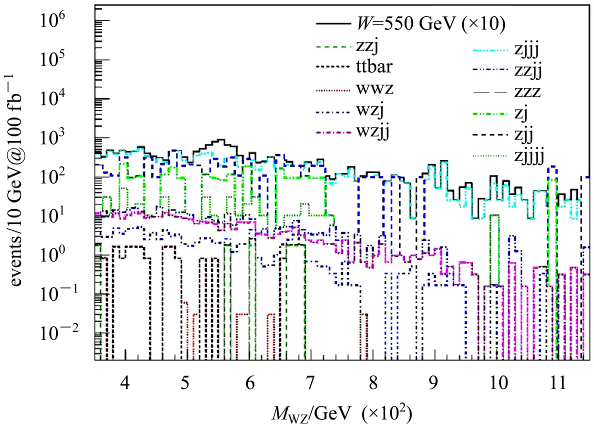

Fig. 5. Distribution of $M_{W^{\pm}Z^0}$ for signal and backgrounds samples at an integrated luminosity of 100 fb^{-1}. All histograms are stacked.

The backgrounds $Z^0+\mathrm{nj}$, $W^{\pm}Z^0\mathrm{jj}$ and $W^{\pm}Z^0\mathrm{j}$ have large contribution to the whole background, while $Z^0Z^0Z^0$, $W^+W^-Z^0$ and $Z^0Z^0\mathrm{j}$ are much smaller backgrounds and almost invisible in the spectrum of $W^{\pm}Z^0$. We estimate the expected sensitivity in mass region of $M_{Z^0W^{\pm}}=M_{W_1^{\pm}}\pm 50$ GeV using the formula

$$S=\sqrt{2\ln Q},\ Q=(1+N_s/N_b)^{N_s+N_b}\exp(-N_s) \quad (6)$$

here N_s and N_b are the events number of the signal and the whole background respectively in each mass region. The expected sensitivity is $3.37\pm0.71\sigma$, which corresponds to 5.0σ for the integrated luminosity of 219.71 ± 92.69 fb^{-1}.

The same procedure with the same selection criteria is applied to the signal process with $M_{W_1^{\pm}}=$ 450, 500, 550, 600, 650, 700, 750, 800 GeV. The remaining events, the significance for 100 fb^{-1} and the integrated luminosity for 5σ detection are shown in Table 4, where the errors represent the effect of systematics and statistics.

Table 4. The number of events (in the mass window $M_{Z^0W^{\pm}}=M_{W_1^{\pm}}\pm 50$ GeV), the significance with the integrated luminosity of 100 fb^{-1} and the integrated luminosity for 5σ signal detection.

$M_{W_1^{\pm}}$/GeV	number of signal (error)	number of bg (error)	σ for 100 fb^{-1} (with sys. error)	lumi(fb^{-1}) for 5σ (with sys. error)
450	230 (27.74%)	8556 (23.24%)	2.52 (0.75)	393.65 (235.56)
500	269 (21.87%)	7803 (23.24%)	3.03 (0.75)	271.86 (133.73)
550	274 (17.83%)	6488 (23.24%)	3.37 (0.71)	219.71 (92.69)
600	113 (17.80%)	5596 (23.24%)	1.50 (0.32)	1108.24 (469.13)
650	79 (26.30%)	4504 (23.24%)	1.17 (0.34)	1814.72 (1040.04)
700	66 (23.58%)	3431 (23.24%)	1.12 (0.29)	1981.71 (1037.95)
750	52 (12.77%)	2191 (23.24%)	1.10 (0.19)	2041.67 (701.02)
800	43 (13.40%)	1478 (23.24%)	1.11 (0.20)	2017.66 (710.86)

4 Systematic uncertainties

The systematic errors we consider here mainly include:

1) The cross section uncertainty for the signal process includes the statistical error and the difference between PDFs CTEQ6L1 [7] and CTEQ6M140 [9] listed in Table 1. The uncertainty of cross sections for backgrounds is assumed to be 20% [10].

2) Due to the initial and final state radiation model, the parton shower and pile-up, the uncertainty is estimated to be 10% [10].

3) The relative uncertainty for lepton identification and reconstruction is assumed 2% [10]. In this process, there are two leptons and the corresponding systematic error for event yield is 4% [4].

4) In the same method as above, the uncertainty for event yield is 0.5% due to 10% uncertainty of lepton p_T resolution [4, 10].

5) The uncertainty is estimated to be 10% for jet energy resolution and 7% for jet energy scale [10]. For the final state with two jets, they bring the uncertainty 2% and 1% respectively for the event yield [4]. So we can obtain 4% and 2% systematic error respectively to this two sources in our process with four jets in the final state.

6) In reconstruction of jet, 5% of them can be identified to be lepton by mistake [10]. In this process, jets faking leptons bring 2% uncertainty to event yield in case of four jets [4].

All the uncertainties of events yields are listed in Table 5 for signal processes and backgrounds samples.

In conclusion, the total uncertainty for remaining event numbers of backgrounds is 23.24% shown in Table 4. Considering the uncertainty of cross sections of signal samples, the total uncertainty for signal samples of every energy region are also shown in Table 4, which contains the errors in Table 5 and the uncertainty of generation cross sections for each sample with different energy region respectively.

Table 5. The uncertainties for event yields common to signal and background samples.

source	uncertainty
parton shower, plie-up	10%
lepton P_t resolution	0.5%
lepton ID efficiency	4%
jet energy scale	4%
jet energy resolution	2%
jets faking leptons	2%

5 Summary

We studied the discovery potential of a new charged boson $W_1^{\pm}$ in the process $pp \to W_1^{\pm}jj \to W^{\pm}Z^0jj \to l^+l^-jjjj$ $(l = e, \mu)$ based on hadronized events with the initial and final state parton showers at the generator level. The signal generator is developed with the Minimal Higgsless Model. As much as possible backgrounds samples are taken into account in background study. The major backgrounds are $pp \to Z^0 + \text{njets}$ and $pp \to W^{\pm}Z^0jj$. Detector effects are also considered. Theoretical and experimental uncertainties are estimated. The integrated luminosity for 5σ signal detection is presented.

Not knowing the real mass of $W_1^{\pm}$, we use the identical selection criteria to select the signal and background events for the various assumed massed of $W_1^{\pm}$ from 450 to 800 GeV. In future, these criteria can be optimized according to the real mass of $W_1^{\pm}$. By this process, the new vector boson $W_1^{\pm}$ may be found in LHC experiments if the mass value is less than 600 GeV, given that it really exists according to the theoretical prediction.

We are grateful to Profs. Y.-P. Kuang and H.-J He for their helpful discussions.

References

1 Chivukula R S, Dicus D A, HE H J. Phys. Lett. B, 2002, **525**: 175; Chivulula R S, HE H J. Phys. Lett. B, 2002, **532**: 121; Csaki C, Grojean C, Murayama H, Pilo L, Terning J. Phys. Rev. D, 2004, **69**: 055006

2 HE H J et al. Phys. Rev. D, 2008, **78**: 031701

3 BIAN J G et al. Nucl. Phys. B, 2009, **819**: 201 [arXiv:0905.2336 (hep-ex)]

4 CHEN M S et al. J. Phys. G: Nucl. Part. Phys., 2009, **36**: 075004

5 Sjöstrand T et al. Comput. Phys. Commun., 2001, **135**: 238

6 Chivukula R S, Coleppa B, Chiara S D, Simmons E H, HE H J, Kurachi M, Tanabashi M. Phys. Rev. D, 2006, **74**: 075011

7 Pumplin J et al. JHEP, 2002, **0207**: 012; Stump D et al. JHEP, 2003, **0310**: 046

8 Alwall J et al. JHEP, 2007, **028A**: 09

9 LAI H L et al. Eur. Phys. J., 2000, **12**: 375

10 The ATLAS Collaboration. Detector and Physics Performance-Technical Design Reports, CERN/LHCC/99-15, vol.1